Published in final edited form as:
Cancer Res. 2013 March 15; 73(6): 1733–1741. doi:10.1158/0008-5472.CAN-12-2384.

Evidence for a role of the PD-1:PD-L1 pathway in immune resistance of HPV-associated head and neck squamous cell carcinoma

Sofia Lyford-Pike[1], **Shiwen Peng**[2], **Geoffrey D. Young**[1,3], **Janis M. Taube**[2,4], **William H. Westra**[1,2], **Belinda Akpeng**[1], **Tullia C. Bruno**[5], **Jeremy D. Richmon**[1], **Hao Wang**[6], **Justin A. Bishop**[2], **Lieping Chen**[7], **Charles G. Drake**[5,8], **Suzanne L. Topalian**[3,5], **Drew M. Pardoll**[5,9], and **Sara I. Pai**[1,5,10]

[1]Department of Otolaryngology-Head and Neck Surgery, Johns Hopkins University School of Medicine and Sidney Kimmel Comprehensive Cancer Center, Baltimore, MD, USA

[2]Department of Pathology, Johns Hopkins University School of Medicine and Sidney Kimmel Comprehensive Cancer Center, Baltimore, MD, USA

[3]Department of Surgery, Johns Hopkins University School of Medicine and Sidney Kimmel Comprehensive Cancer Center, Baltimore, MD, USA

[4]Department of Dermatology, Johns Hopkins University School of Medicine and Sidney Kimmel Comprehensive Cancer Center, Baltimore, MD, USA

[5]Department of Oncology, Johns Hopkins University School of Medicine and Sidney Kimmel Comprehensive Cancer Center, Baltimore, MD, USA

[6]Department of Biostatistics, Johns Hopkins University School of Medicine and Sidney Kimmel Comprehensive Cancer Center, Baltimore, MD, USA

[7]Department of Immunobiology, Yale University School of Medicine, New Haven, CT, USA

[8]Department of Urology, James Buchanan Brady Urological Institute, Johns Hopkins University School of Medicine, Baltimore, MD, USA

[9]Immunology and Hematopoiesis Division, Sidney Kimmel Comprehensive Cancer Center, Baltimore, MD, USA

Abstract

Human papillomavirus-associated head and neck squamous cell carcinomas (HPV-HNSCC) originate in the tonsils, the major lymphoid organ that orchestrates immunity to oral infections. Despite its location, the virus escapes immune elimination during malignant transformation and progression. Here, we provide evidence for the role of the PD-1:PD-L1 pathway in HPV-HNSCC immune resistance. We demonstrate membranous expression of PD-L1 in the tonsillar crypts, the site of initial HPV infection. In HPV-HNSCCs that are highly infiltrated with lymphocytes, PD-L1 expression on both tumor cells and CD68+ tumor associated macrophages (TAMs) is geographically localized to sites of lymphocyte fronts, while the majority of CD8+ tumor infiltrating lymphocytes (TILs) express high levels of PD-1, the inhibitory PD-L1 receptor. Significant levels of mRNA for interferon-γ (IFN-γ), a major cytokine inducer of PD-L1

[10]Corresponding author and to whom proofs and reprint requests should be sent: Sara I. Pai, MD, PhD 601 N. Caroline Street, JHOC 6th floor Baltimore, MD 21287 Phone: 410-502-9825 Fax: 410-955-0035 spai@jhmi.edu.

Disclosures: Drs. Charles Drake and Suzanne Topalian have served as consultants to Bristol-Myers Squibb (BMS). Dr. Drake has licensed patents to BMS. Dr. Topalian has received research grants from BMS.

expression, were found in HPV+ PD-L1(+) tumors. Our findings support the role of the PD-1:PD-L1 interaction in creating an "immune-privileged" site for initial viral infection and subsequent adaptive immune resistance once tumors are established and suggest a rationale for therapeutic blockade of this pathway in patients with HPV-HNSCC.

Keywords

PD-1; PD-L1; immune checkpoint; adapative resistance; HPV; head and neck cancers; oropharyngeal cancers; squamous cell carcinomas

INTRODUCTION

Human papillomavirus (HPV) is recognized as the causative agent of a growing subset of head and neck cancers (1, 2). It is now estimated that HPV is responsible for up to 80% of oropharyngeal cancers in the United States (3, 4). HPV-associated head and neck squamous cell carcinomas (HPV-HNSCC) differ from tobacco-related head and neck cancers in several ways (5, 6). The patients tend to be younger in age, lack a significant tobacco and/or alcohol history, and have improved clinical outcomes. The virus-related tumors arise from the deep crypts within the lymphoid tissue of the tonsil and base of tongue and the majority can be distinguished from tobacco-related head and neck cancers by the characteristic infiltration of lymphocytes in the stroma and tumor nests (7). Nevertheless, despite this profound inflammatory response, HPV-HNSCCs are able to evade immune surveillance, persist, and grow.

Various mechanisms have been proposed for the resistance of human solid tumors to immune recognition and obliteration, including the recruitment of regulatory T cells, myeloid derived suppressor cells, and local secretion of inhibitory cytokines. Recent evidence suggests that tumors co-opt physiologic mechanisms of tissue protection from inflammatory destruction via up-regulation of immune inhibitory ligands; this has provided a new perspective for understanding tumor immune resistance. Antigen-induced activation and proliferation of T cells are regulated by the temporal expression of both co-stimulatory and co-inhibitory receptors and their cognate ligands. Coordinated signaling through these receptors modulates the initiation, amplification and subsequent resolution of adaptive immune responses. In the absence of co-inhibitory signaling, persistent T cell activation can lead to excessive tissue damage in the setting of infection as well as autoimmunity. In the context of cancer, in which immune responses are directed against antigens specifically or selectively expressed by tumor cells, these immune checkpoints can represent major obstacles to the generation and maintenance of clinically meaningful anti-tumor immunity. Therefore, efforts have been made in the clinical arena to investigate blockade of immune checkpoints as a novel therapeutic approach to cancer. CTLA-4 and programmed cell death-1 (PD-1) are two such checkpoint receptors being actively targeted in the clinic. Ipilimumab, a monoclonal antibody (mAb) that blocks CTLA-4, demonstrated an overall survival benefit in patients with advanced metastatic melanoma in a randomized phase III clinical trial; however, it was associated with significant immune-related toxicities (8). In a first-in-human clinical trial, a blocking mAb against PD-1 (BMS-936558, MDX-1106/ONO-4538) was evaluated in patients with advanced metastatic melanoma, colorectal cancer, castrate-resistant prostate cancer, non-small-cell lung cancer (NSCLC), and renal cell carcinoma (RCC). In this study, the antibody was well-tolerated and there was evidence of clinical activity in all of the evaluated histologies except prostate cancer (9). In a subset of patients, tumor cell surface or "membranous" expression of the major PD-1 ligand, PD-L1, appeared to correlate with the likelihood of response to therapy. Expanded phase I clinical studies with anti-PD-1(BMS-936558) and anti-PD-L1 (BMS-936559) confirmed objective

clinical responses in RCC, melanoma, and NSCLC, and again a relationship between tumor cell surface PD-L1 expression and objective responses to anti-PD-1 therapy was observed (10, 11).

Given the promising safety profile and clinical responses observed in blocking the PD-1 immune checkpoint, we evaluated the role of the PD-1:PD-L1 pathway in HPV-HNSCC. These investigations are aimed at understanding how HPV can infect a lymphoid rich organ, such as the tonsil, and yet still evade immune clearance as it induces malignant transformation of infected cells. Our findings support a model in which the PD-1:PD-L1 pathway creates an immune privileged site for HPV infection and becomes further induced during the subsequent development of HPV-HNSCC as an adaptive resistance mechanism of tumor against host.

MATERIALS AND METHODS

Human Subjects

Patients undergoing surgical resection for tonsil (palatine or lingual) cancer were enrolled in this study that was approved by the Johns Hopkins Institutional Review Board, after providing informed consent. HPV status was determined by in situ hybridization (ISH) and p16 immunohistochemistry (IHC). Briefly, 5 uM sections from formalin-fixed paraffin embedded (FFPE) tumor blocks were evaluated with the Ventana HPV III Family16 probe set. Punctate hybridization signals localized to tumor cell nuclei defined a HPV-positive tumor. P16 expression was evaluated using the Ultra view polymer detection kit (Ventana Medical Systems, Inc. Tucson, AZ) on a Ventana BenchmarkXT autostainer (Ventana); expression was scored as positive if strong and diffuse nuclear and cytoplasmic staining was present in ≥70% of the tumor. All slides were interpreted by a head and neck pathologist (WHW).

A separate cohort of patients (both adults and pediatric patients, <2 years of age) undergoing a tonsillectomy for management of a non-malignant process such as tonsil hypertrophy or chronic tonsillitis served as non-cancer controls.

Flow Cytometry Analysis

Circulating peripheral blood mononuclear cells (PBMCs) isolated by density gradient centrifugation and infiltrating lymphocytes dissociated from fresh tumor or non-malignant tonsil digests were stained with the following mAbs: anti-human CD3-PERCP, CD8-APC, CD4-FITC (BD Biosciences, Mountain View, CA), and anti-human PD-1 (MDX-1106, fully human IgG4, 10 ug/ml, BMS, New York, NY) or an isotype control, anti-diphtheria toxin human IgG4 (BMS). Anti-human IgG4-PE (SouthernBiotech, Birmingham, AL) was used as a secondary label. Analysis was performed on FACSCalibur (BD Biosciences) with CELLQuest or Flow Jo software (BD Biosciences and Tree Star Inc, Ashland, OR, respectively).

Flow cytometric analysis of PD-L1 expression in four HNSCC cell lines (JHU011, JHU022, JHU028, JHU029) was performed. Subconfluent cells were treated with 10 ng/ml of recombinant human interferon-gamma-(IFN-γ) (Peprotech, NJ) or were untreated. After 24 hours, the cells were harvested and stained with either mouse anti-human PD-L1 (clone 5H1) or a mouse IgG1 isotype control, followed by PE-conjugated goat anti-mouse Ig. The cells were acquired with FACSCalibur and analyzed with CellQuest Pro software.

PD-L1 and PD-1 Detection by Immunohistochemistry

PD-L1 expression analysis was performed using mAb 5H1 as previously described (9, 12). Briefly, FFPE tissue sections were deparaffinized and dehydrated in xylene and graded ethanol solutions. Antigen retrieval was performed in Tris-EDTA buffer and the DAKO Catalyzed Signal Amplification System for mouse antibodies was used for staining and detection (DAKO, Carpinteria, CA). Mouse IgG1 isotype matched control antibody and secondary biotinylated anti-mouse IgG1 antibody were used (BD Biosciences). PD-L1 expression in deep crypts and germinal centers in non-tumor involved areas of lymphoid tissue served as an internal positive control. A 5% threshold of cell surface PD-L1 expression on tumor cells was defined as positive (12).

For PD-1 immunostaining, the murine anti-human PD-1 mAb, clone M3, was used. Citrate buffer (pH 6.0) was used for antigen retrieval, and a CSA System (DAKO; Glostrup, Denmark) was used for signal amplification, followed by development with diaminobenzidine chromagen. All slides were reviewed and interpreted independently by two pathologists (WHW and JT).

Detection of Immune Cell Infiltrates in Tonsil Cancers

Serial 5 uM tissue sections were immunostained with anti-CD3, CD4, CD8, CD68 or CD1a using the Ultraview polymer detection kit (Ventana Medical Systems) on a Ventana BenchmarkXT autostainer (Ventana Medical Systems) under a standard protocol with isotype control antibodies by the Pathology Core Laboratory at Johns Hopkins Hospital. The intensity of the infiltrate was graded as 0 (none), 1 (mild, perivascular infiltrate), 2 (moderate, perivascular infiltrate extending away from vessels and into tumor), or 3 (severe or diffuse lymphocytic infiltrate throughout the tumor). This grading system was adapted from previously published work (12).

Quantitative RT-PCR

Frozen oropharyngeal tumor specimens were scraped from glass slides with a sterile scalpel and total RNA was isolated using the Qiagen RNeasy Micro Kit (Qiagen, Valencia CA). 50 ng of total RNA from each specimen was reverse-transcribed in a 10 ul reaction volume using qScript cDNA SuperMix (Quanta Biosciences, Gaithersburg MD) per protocol. 0.5 ul from each RT reaction was combined with 5ul TaqMan Universal Master Mix II (Applied Biosystems, Foster City CA), 4ul Molecular Grade Water, and 0.5 ul of primer/probe preparations specific for human IFN-γ, CD8a, CD4, or GAPDH (Applied Biosystems). PCR reactions were run in triplicate on 384-well plates using a 7900 HT Fast Real Time PCR system (Applied Biosystems). Cycle thresholds were determined using a manual cutoff of 0.04. The assay was performed in duplicate.

Evaluation of PTEN Expression

Total protein was extracted from four HPV-negative HNSCC cell lines (JHU011, JHU022, JHU028, JHU029) using a M-PER mammalian protein extraction reagent (Thermo Scientific, Rockford, IL) in the presence of a protease inhibitor cocktail (Roche, Germany), and was loaded onto a 10% SDS-PAGE gel. After membrane blotting, the expression of PTEN was detected with the rabbit anti-PTEN mAb D4.3 (Cell Signaling, Beverly, MA) followed by incubation with goat anti-rabbit IgG conjugated to horseradish peroxidase. Expression of PTEN protein was visualized using an Amersham ECL western blotting detection reagent (GE Health, Pittsburgh, PA). The HeLa cell line was used as positive control for PTEN expression and β-actin was used as a loading control. All of these cell lines were generated at Johns Hopkins Medical Institutions and authenticated by genomic sequencing.

Intracellular IFN-γ Functional Assay

After exclusion of dead cells with the Live/Dead Fixable Acqua Dead Cell Staining Kit (Invitrogen Molecular Probes, Eugene, OR), lymphocytes (PBMCs, TILs) were incubated with anti-human mAbs for CD45RO-APC-H7 (BD Biosciences), CD3-efluor 450, CD8-Pe-Cy7 (eBioscience), and anti-PD1 mAb MDX-1106 and its secondary anti-IgG4-PE (Southern Biotech, Birmingham, AL). CD45RO+CD3+CD8+ T cells were sorted based on PD-1 expression by FACSAria (Becton Dickinson, San Jose, CA). Cells were stimulated for 6 hours with phorbol 12-myristate 13-acetate (PMA) and ionomycin in the presence of Golgi Stop (BD Biosciences). Cells were then fixed, permeabilized (Foxp3 Fixation/ Permeabilization Concentrate and Diluent, eBioscience) and stained for intracellular cytokines (IFNγ-PerCP-Cy5.5 and TNFα-APC). Analysis was performed on LSRII with FACSDiva software (Becton Dickinson).

Statistical Analysis

Statistical significance of PD-1 expression by CD4 and CD8 lymphocytes was evaluated using the Student's t-test. For the qRT-PCR assays, a Fisher's exact test was used. For the functional assays, T cell cytokine expression was log transformed, and comparisons of expression between PD-1 (+) and (-) T cells were evaluated by fold-difference. Mixed effect models were used to take into account correlations within the same subject. To compare the differential expression of PD-1 (+) vs. PD-1(-) T cells between sample types, we tested the interaction between the PD-1 status and sample type (HNSCC and PBMC) in the model.

RESULTS AND DISCUSSION

Localized expression of PD-L1 within deep tonsillar crypts, the site of initial HPV infection and origin of HPV-HNSCC

HPV-HNSCC localizes to the lingual and palatine tonsils – lymphoepithelial organs that represent a first line of defense against oral infections. Paradoxically, oncogenic HPVs express foreign viral antigens that are capable of eliciting robust immune responses, but are none-the-less able to escape immune clearance. To explore potential mechanisms for immune resistance, we evaluated expression of PD-L1 in non-cancerous adult tonsil tissue and HPV naïve pediatric patients and found localized expression of PD-L1 to the reticulated epithelium of the deep crypts, which are the sites of origin of these virus-related cancers **[Figure 1A]**. Interestingly, we did not find PD-L1 expression on the surface epithelium of tonsils **[Figures 1B and C].** This suggests that the reticulated epithelium of tonsillar crypts may represent a distinct immune microenvironment relative to the surface epithelium. The deep invagination of tonsil crypts makes them susceptible to collection of bacteria and foreign material. Thus, the resident lymphohistiocytes are chronically exposed to high concentrations of foreign antigen. It is therefore possible that, even in the absence of overt chronic tonsillitis, there is ongoing basal immune activation in the crypts driving PD-L1 expression. Given the selective expression of PD-L1 within the deep crypts, this region may consequently represent an immune-privileged site, in which effector function of virus-specific T cells is down-modulated, thereby facilitating immune evasion at the time of initial HPV infection and subsequent virus-induced malignant transformation.

Programmed Death-1 (PD-1) receptor expressed by CD8+ TILs in HPV-HNSCC

In order to further evaluate the relevance of the PD-1:PD-L1 pathway in the development of HPV-HNSCC, we compared the frequency of PD-1 expression on TILs and PBMCs isolated from patients with HPV-HNSCC vs. patients with a non-malignant tonsil process. We found that PD-1 expression by both CD4+ and CD8+ T cells was higher in tonsil tissue as compared to the peripheral blood of patients with either HPV-HNSCC or with benign,

chronically inflamed tonsils (all $p < 0.05$; **Figures 2A and B**). There was no significant difference in the frequency of PD-1 expressing CD4+ T cells infiltrating tumors vs. benign tonsils ($p=0.31$) (**Figure 2A**). However, there was a higher frequency of PD-1 expression on CD8+ TILs (mean frequency 73.5%, SD 14.1) vs. CD8+ T cells in benign, chronically inflamed tonsils (mean frequency 35.5%, SD 13.4 $p<0.0001$) (**Figure 2B**). Strikingly, CD8+ TILs from HPV-HNSCC contained a distinct population of PD-1^{hi} cells not observed among CD8+ T cells from inflamed tonsils.

Patterns of PD-L1 expression in the tumor microenvironment of HPV-HNSCC

In normal tissue, PD-1 ligands are induced in response to inflammatory cytokines such as IFN-γ. This system represents a major mechanism for tissue protection in the setting of T cell-mediated inflammation. We therefore sought to determine whether expression of the major PD-1 ligand, PD-L1, is linked to infiltrating TILs and IFN-γ production. We evaluated PD-L1 expression in HPV-HNSCC by IHC and initially correlated expression with TIL infiltration and the presence of HPV DNA **(Figures 3A-D)**.

Two patterns of cellular distribution of PD-L1 have been described: membranous (cell surface) and cytoplasmic (9, 12, 14). Among 20 HPV-HNSCC samples examined in our study, 14 (70%) expressed PD-L1 and all of these (14 of 14) displayed cell surface staining on ≥5% of tumor cells. Furthermore, we found that nearly all (13 of 14) demonstrated staining restricted to the tumor periphery at the interface between tumor cell nests and inflammatory stroma (**Figures 3D and E)**, whereas only 1 of 14 demonstrated diffuse PD-L1 expression throughout the tumor nests (**Figure 3F, Table 1**).

In order to determine if PD-L1 expression was specific to HPV-HNSCC, we evaluated 7 HPV-negative tonsil cancers and found that only 29% (2 of 7) expressed PD-L1. PD-L1 expression in HPV-negative cancers was membranous and at the tumor periphery juxtaposed to immune infiltrates, similar to HPV-HNSCC (**Table 1**).

Association of PD-L1 expression with TILs and co-localization with tumor associated macrophages

All sixteen PD-L1-expressing HPV(+) and HPV(-) tumors were detected in the setting of a host inflammatory immune response (grades 1-3), indicating an association of PD-L1 expression with the presence of TILs (**Table 1**). In contrast, among 11 PD-L1(-) tumors, 5 (45%) contained TILs. These results suggest that TILs are necessary but not sufficient to induce tumor cell PD-L1 expression ($p = 0.0016$, Fisher's exact test) and imply that the functional profile of TILs may be an important determining factor.

Given the geographic heterogeneity of membranous PD-L1 expression within the tumor microenvironment, we wanted to determine the spatial relationship of infiltrating immune cells to PD-L1 expression. CD3+, CD4+, and CD8+ T lymphocytes were found to intercalate among tumor cells **(Figure 4A-D)**. We did not observe any difference in the density or quality of TILs between the two patterns of PD-L1 expression (peripheral vs. diffuse throughout the tumor). We found that in 6 of 9 PD-L1-expressing tumors, there were equal or greater proportions of CD8+ T cells infiltrating the tumor and stroma as compared to CD4+ T cells. The majority of these CD8+ T cells expressed the PD-1 receptor (mean frequency 73.5%, SD 14.1) (**Figure 2B**). For those tumors that demonstrated PD-L1 expression at the tumor periphery, the CD8+ T cells were juxtaposed to PD-L1 expressing cells.

Membranous PD-L1 expression was localized to tumor as well as inflammatory cells. In order to further characterize the immune cells expressing PD-L1, IHC for cells of the

macrophage lineage with anti-CD68, and for interdigitating dendritic cells with anti-CD1a, was performed. CD1a did not co-localize with PD-L1 (data not shown). However, CD68 co-localized with the two observed patterns of membranous PD-L1 expression, peripheral or diffuse, in the tumor microenvironment **(Figures 4E and F)**. PD-L1+CD68+ tumor associated macrophages (TAMs) at the interface between the tumor periphery and the surrounding inflammatory stroma may create a PD-L1 immunoprotective "barrier" around the tumor nests. These findings suggest that there are multiple cell types expressing PD-L1 within the tumor microenvironment of HPV-HNSCC, including a mixture of epithelial-derived tumor cells, and recruited CD68+ TAMs. Furthermore, they suggest an adaptive resistance mechanism whereby PD-L1 expression by tumor cells and host infiltrating TAMs is induced by inflammatory signals, setting up a local interaction in the microenvironment between T cells expressing PD-1 receptor and its ligand, PD-L1 **(Figures 4D and E)**.

In hepatocellular carcinoma (HCC), it has been reported that PD-L1 overexpression is associated with TAM infiltration, suggesting that overexpression of PD-L1 may be induced by an inflammatory microenvironment involving macrophages (16). Zhao et al reported that PD-L1(+) macrophages were enriched predominantly in the peritumoral stroma of HCC and that IL-17 could activate monocytes as well as hepatoma cells to express PD-L1 (17). Here, we demonstrate that PD-L1 co-localizes with CD68+ TAMs in HPV-HNSCC and we hypothesize that macrophages may be mediators of adaptive resistance through the PD-1:PD-L1 pathway to dampen tumor specific T cell functions. Further investigation is needed to evaluate the immune signatures and identify the players critical to recruiting or driving PD-L1 expression at the tumor interface.

Interferon-γ upregulates PD-L1 expression

The co-localization of lymphocytic infiltrates and PD-L1 expression, together with the defined role of IFN-γ in inducing PD-L1 expression by tumor cells, led us to explore IFN-γ expression in the microenvironment of HPV-HNSCC. Quantitative RT-PCR was performed for IFN-γ as well as the leukocyte antigens CD4 and CD8 in PD-L1(+) and PD-L1(-) oropharyngeal tumors (**Figure 5**). We found a significant increase in expression of CD8 ($p=0.002$) and IFN-γ ($p=0.003$) mRNA in PD-L1(+) as compared to PD-L1(-) cancers. No significant difference in expression was observed for CD4+ T cells ($p=0.08$) or GAPDH ($p=0.96$). This suggests that CD8+ TILs present in PD-L1(+) HPV-HNSCC are activated and secrete IFN-γ, which may be driving the expression of PD-L1 at the tumor fronts juxtaposed to the inflammatory stroma (**Figures 4D and E)**.

These findings are highly compatible with a model in which IFN-γ and potentially other cytokines associated with an immune response induce PD-L1 on tumor cells, which then down-modulates anti-tumor immunity to an extent which facilitates tumor survival.

In addition to this adaptive resistance mechanism, oncogene driven "innate" PD-L1 expression represents an alternative mechanism. For example, PD-L1 expression has been reported to increase with PI3 kinase/AKT pathway activation due to loss of phosphatase and tensin homolog (PTEN) function in glioblastoma cells (18). However, PTEN loss is rarely observed in HPV(+) HNSCC (19-21) so it is unlikely to be relevant to PD-L1 induction observed in this subset of cancers. However, PTEN loss is more common among HPV(-) HNSCC. Indeed, four of four HPV(-) HNSCC cell lines had lost PTEN expression as assessed by Western blot, and 3 of 4 cell lines expressed endogenous levels of PD-L1 (**Supplemental File 1A**). When IFN-γ was added to the cultures, the PD-L1(-) cell line demonstrated surface PD-L1 induction and the three lines with baseline PD-L1 expression demonstrated at least a 10-fold up-regulation of surface PD-L1 (**Supplemental File 1B**). These findings suggest that, as with other cancer types, innate and adaptive mechanisms of PD-L1 expression can be simultaneously operative.

PD-1 expressing CD8+ TILs are functionally anergic relative to peripheral blood PD-1 expressing T cells

While PD-L1 expression on HNSCC is variable, PD-1 is always expressed on a high proportion of TILs – much higher than on peripheral blood T cells (**Figure 2** and data not shown). It was therefore of interest to determine the functional capacity of PD-1(+) TILs in relation to patient-matched peripheral T cells. In the peripheral blood, CD45RO +CD3+CD8+PD-1(+) T cells demonstrated enhanced IFN-γ production in response to PMA/ionomycin stimulation, as compared to CD45RO+CD3+CD8+PD-1(-) T cells (mean ratio 4.04) in all four HPV-HNSCC patients evaluated **(Figures 6A and B, Supplemental File 2)**. This is consistent with the concept that PD-1 expression on peripheral T cells marks antigen-experienced effector and memory cells, not exhausted or anergic cells. In striking contrast, CD45RO+CD3+CD8+PD-1(+) TILs demonstrated a decreased ability to produce IFN-γ as compared to the CD45RO+CD3+CD8+PD-1(-) TILs (mean ratio 0.84) **(Figures 6A and B, Supplemental File 2)**. This difference in IFN-γ production between the PD-1(+) and PD-1(-) TILs compared to peripheral blood T cells was highly significant (p=0.005) and suggested PD-1 expression within the tumor microenvironment marks TILs that are functionally suppressed in their capacity to produce effector cytokines and may be indeed at least partially responsible for this suppression. Similar functional assays were performed for tumor necrosis factor (TNF)-α production and, again, a decrease in functional ability of the CD8+PD-1(+) TILs to produce TNF-α as compared to CD8+PD-1(-) TILs was observed (mean ratio 0.69, SD 0.7). However, in the peripheral blood, we did not observe a decreased ability of CD8+PD-1(+) T lymphocytes to produce TNF-α as compared to CD8+PD-1(-) T cells (mean ratio 1.26, SD 0.14).

We also compared the functional status of CD8+ PD-1(+) vs. CD8+PD-1(-) T cells in the peripheral blood and tissue of chronic tonsillitis patients. In contrast to TILs from cancer patients, we did not observe significant differences in the functional capacity of PD-1(+) vs. PD-1(-) tissue infiltrating CD8+ T cells, or between circulating vs. tissue infiltrating CD8+ PD-1(+) T cells (mean ratio 1.49 (SD 0.86) vs. 1.05 (SD 0.35), respectively, p=0.61, **Supplemental File 3**). This finding further supports the distinct immune inhibitory role of the PD-1 pathway within the tumor microenvironment as opposed to inflammation in the non-cancerous setting, where PD-1 expression likely marks activated cells whose functional capacity is not impaired.

HPV-HNSCCs have favorable clinical outcomes with survival rates of 82% at 3 years, compared to 57% in non-HPV-HNSCCs (6). Improved survival has been attributed to a younger patient age and enhanced tumor responsiveness to chemoradiation therapy. However, a contributing factor may also be the strong host immune response generated against these tumors. Evidence for inherent immunologic responses generated against HPV-HNSCC is the observed high frequency of TILs and inflammatory responses within these tumors. Indeed, HPV-HNSCC express foreign viral proteins, such as the E6 and E7 antigens, for which the host immune system should not be tolerant. Similar favorable clinical outcomes in the presence of TILs have been observed with other solid tumors including ovarian, esophageal, small cell lung, and colorectal cancers (22-25). While strong host immune responses may account for favorable clinical outcomes, the findings presented here suggest that these local immune responses induce the PD-1:PD-LI checkpoint pathway, which in turn may limit the capacity of TILs to ultimately eliminate the tumor without therapeutic intervention. The relevance of the PD-1:PD-L1 checkpoint in cancer immunity is highlighted by reports demonstrating that blockade of PD-L1 or PD-1 by specific mAbs can reverse the anergic state of tumor-specific T cells and thereby enhance antitumor immunity (10-11, 26-27).

We propose here that the PD-1:PD-L1 pathway plays a role in both persistence of HPV infection (through expression of PD-L1 in the tonsillar crypt epithelium – the site of initial infection) as well as resistance to immune elimination during malignant progression. These findings extend those recently reported in melanoma (12), which is a non-virus associated cancer but has also been considered to be "immunogenic." Similar to melanoma, and in keeping with the proposed adaptive resistance hypothesis, PD-L1 is not expressed uniformly within HPV-HNSCCs but rather at sites of lymphocyte infiltration. In contrast to melanoma, in which approximately 40% of tumors express PD-L1, the majority of HPV-HNSCC tumors (70%) and a subset of HPV-negative HNSCC (29%) are PD-L1(+). The few PD-L1(-) tumors, that are lymphocyte poor, have a different immune microenvironment with potential activation of alternative mechanisms of immune resistance.

Given the high levels of membranous PD-L1 expression within the tumors, our studies support a rationale for administering PD-1/PD-L1 targeted therapy to the HPV-HNSCC patient population. Future studies will need to validate these findings in a larger cohort, characterize the gene signatures of tumor immune infiltrates associated with PD-L1 expression, and identify additional factors responsible for inducing local PD-L1 expression and hence immunosuppression within the tumor microenvironment.

Supplementary Material

Refer to Web version on PubMed Central for supplementary material.

Acknowledgments

GRANT SUPPORT

This work was supported by the NIH/NIDCR P50 DE019032 Head and Neck Cancer SPORE grant (WHW, SIP), NIH/NIDCD T32000027 grant (SLP), and NIH R01 CA142779 (SLT).

REFERENCES

1. Gillison ML, Koch WM, Capone RB, Spafford M, Westra WH, Wu L, et al. Evidence for a causal association between human papillomavirus and a subset of head and neck cancers. J Natl Cancer Inst. 2000; 92(9):709–20. [PubMed: 10793107]
2. Chaturvedi, Ak; Engels, EA.; Pfeiffer, RM.; Hernandez, BY.; Xiao, W.; Kim, E., et al. Human papillomavirus and rising oropharyngeal cancer incidence in the United States. J Clin Oncol. 2011; 1029(32):4294–301. [PubMed: 21969503]
3. Begum S, Cao D, Gillison M, Zahurak M, Westra WH. Tissue distribution of human papillomavirus 16 DNA integration in patients with tonsillar carcinoma. Clin Cancer Res. 2005; 11(16):694–9.
4. Singhi AD, Westra WH. Comparison of human papillomavirus in situ hybridization and p16 immunohistochemistry in the detection of human papillomavirus-associated head and neck acner based on a prospective clinical experience. Cancer. 2010; 116(9):2166–73. [PubMed: 20186832]
5. Gillison ML, D'Souza G, Westra W, Sugar E, Xiao W, Begum S, et al. Distinct risk factor profiles for human papillomavirus type 16-positive and human papilomavirus type 16-negative head and neck cancers. J Natl Cancer Inst. 2008; 100(6):407–20. [PubMed: 18334711]
6. Ang KK, Harris J, Wheeler R, Weber R, Rosenthal DI, Nguyen-Tan PF, et al. Human papillomavirus and survival of patients with oropharyngeal cancer. N Engl J Med. 2010; 363(1):24–35. [PubMed: 20530316]
7. Westra WH. The changing face of head and neck cancer in the 21st century: the impact of HPV on the epidemiology and pathology of oral cancer. Head Neck Pathol. 2009; 1:78–81. [PubMed: 20596995]
8. Hodi FS, O'Day SJ, McDermott DF, Weber RW, Sosman JA, Haanen JB, et al. Improved survival with ipilumimab in patients with metastatic melanoma. N Engl J Med. 2010; 363:711–23. [PubMed: 20525992]

9. Brahmer JR, Drake CG, Wollner I, Powderly JD, Picus J, Sharfman WH, et al. Phase I study of single-agent anti-programmed death-1 (MDX-1106) in refractory solid tumors: safety, clinical activity, pharmacodynamics, and immunologic correlates. J Clin Oncol. 2010; 28:2167–75. [PubMed: 20351334]
10. Topalian SL, Hodi FS, Brahmer JR, Gettinger SN, Smith DC, McDermott DF, et al. Safety, activity, and immune correlates of anti-PD-1 antibody in cancer. N Eng J Med. 2012; 366(26): 2443–54.
11. Brahmer JR, Tykodi SS, Chow LQM, Hwu WJ, Topalian SL, Hwu P, et al. Safety and activity of anti-PD-L1 antibody in patients with advanced cancer. N Eng J Med. 2012; 366(26):2455–65.
12. Taube JM, Anders RA, Young GD, Xu H, Sharma R, McMiller TL, et al. Colocalization of inflammatory response with B7-H1 expression in human melanocytic lesions supports an adaptive resistance mechanism of immune escape. Sci Transl Med. 2012; 4(127):127–37.
13. Dong H, Strome SE, Salomao DR, Tamura H, Hirano F, Flies DB, et al. Tumor-associated B7-H1 promotes T-cell apoptosis: a potential mechanism of immune evasion. Nat Med. 2002; 8:793–800. [PubMed: 12091876]
14. Strome SE, Dong H, Tamura H, Voxx SG, Flies DB, Tamada K, et al. B7-H1 blockade augments adoptive T-cell immunotherapy for squamous cell carcinoma. Cancer Res. 2003; 63:6501–05. [PubMed: 14559843]
15. Peng S, Lyford-Pike S, Akpeng B, Wu A, Hung CF, Hannaman D, et al. Low-dose cyclophosphamide administered as daily or single dose enhances the antitumor effects of a therapeutic HPV vaccine. Cancer Immunol Immunother. Aug 4.2012 [Epub ahead of print].
16. Chen J, Li G, Meng H, Fan Y, Song Y, Wang S, et al. Upregulation of B7-H1 expression is associated with macrophage infiltration in hepatocellular carcinomas. Cancer Immunol Immunother. 2012; 61(1):101–8. [PubMed: 21853301]
17. Zhao Q, Xiao X, Wu Y, Wei Y, Zhu LY, Zhou J, et al. Interleukin-17-educated monocytes suppress cytotoxic T cell function through B7-H1 in hepatocellular carcinoma patients. Eur J Immunol. 2011; 41:2314–22. [PubMed: 21674477]
18. Parsa AT, Waldron JS, Panner A, Crane CA, Parney IF, Barry JJ, et al. Loss of tumor suppressor PTEN function increases B7-H1 expression and immunoresistance in glioma. Nat Med. 2007; 13(1):84–8. [PubMed: 17159987]
19. Won HS, Jung CK, Chun SH, Kang JH, Kim YS, Sun DI, et al. Difference in expression of EGFR, pAkt, and PTEN between oropharyngeal and oral cavity squamous cell carcinoma. Oral Oncol. 2012; 48(1):985–990. [PubMed: 22682934]
20. Agrawal N, Frederick MJ, Pickering CR, Gettegowda C, Chang K, Li RJ, et al. Exome sequencing of head and neck squamous cell carcinoma reveals inactivating mutations in NOTCH1. Science. 2011; 333(6046):1154–7. [PubMed: 21798897]
21. Stransky N, Egloff AM, Tward AD, Kostic AD, Cibulskis K, Sivachenko A, et al. Science. 2011; 333(6046):1157–60. [PubMed: 21798893]
22. Eerola, Ak; Soini, Y.; Paakko, P. A high number of tumor infiltrating lymphocytes are associated with a small tumor size, low tumor stage, and a favorable prognosis in operated small cell lung carcinoma. Clin Can Res. 2000; 6:1875–81.
23. Schumaher K, Haensch W, Roefzaad C, Schlag PM. Prognostic significance of activated CD8(+) T cell infiltrations within esophageal carcinomas. Cancer Res. 2001; 61:3932–6. [PubMed: 11358808]
24. Zhang L, Conejo-Garcia JR, Katsarors D, Gimotty PA, Massobrio M, Regnani G, et al. Intratumoral T cells, recurrence, and survival in epithelial ovarian cancer. N Engl J Med. 2003; 348:203–13. [PubMed: 12529460]
25. Galon J, Costes A, Sanchez-Cabo F, Kirilovsky A, Mlecnik B, Lagorce-Pages C, et al. Type, density, and location of immune cells within human colorectal tumors predict clinical outcome. Science. 2006; 313:1960–4. [PubMed: 17008531]
26. Hirano F, Kaneko K, Tamura H, Dong H, Wang S, Ichikawa M, et al. Blockade of B7-H1 and PD-1 by monoclonal antibodies potentiates cancer therapeutic immunity. Cancer Res. 2005; 65(3): 1089–96. [PubMed: 15705911]

27. Porichis F, Kwon DS, Zupkosky J, Tighe DP, McMullen A, Brockman MA, et al. Responsiveness of HIV-specific CD4 T cells to PD-1 blockade. Blood. 2011; 118(4):965–74. [PubMed: 21652684]

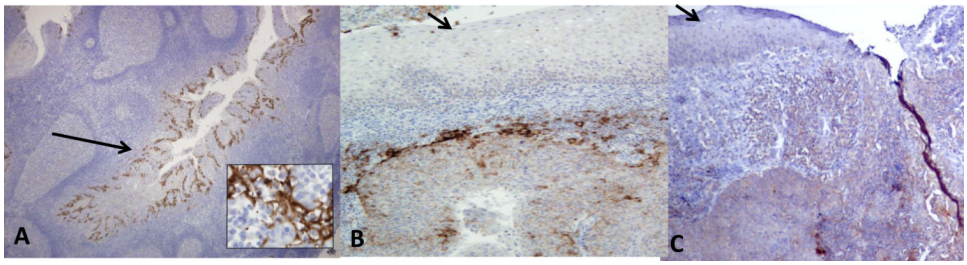

Figure 1. The reticulated epithelium of benign tonsil tissue expresses high levels of PD-L1

A. Chronically inflamed tonsil tissue demonstrates localized PD-L1 expression within the reticulated epithelium of tonsillar crypts (long arrow). Magnification, x40. The inset (magnification, x400) demonstrates cell surface staining of the crypt epithelial cells. In contrast, the surface epithelium of the tonsils was negative for PD-L1 expression (short arrows) (**B, C)**. Magnification, x40.

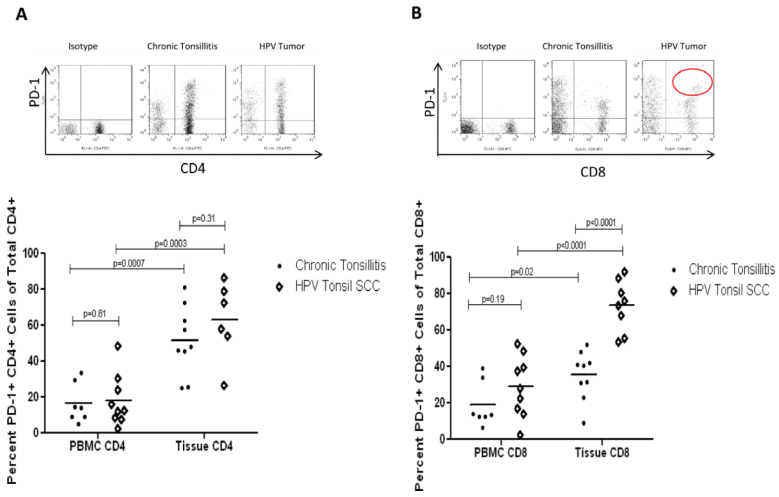

Figure 2. High levels of PD-1 receptor on TILs from HPV-HNSCC

A. Representative flow cytometry of CD4+ T cell population expressing PD-1 in various tissues. Summary graph with mean frequency of CD4+PD-1(+) T cells in non-cancerous tonsils and HPV-HNSCC as compared to peripheral blood. **B**. Similar analysis performed for CD8+PD-1(+) T cell population. The circle on the representative flow data highlights a subpopulation of CD8+ TILs with high levels of PD-1 expression which was not observed in benign tonsils. (•) denotes chronic tonsillitis specimens and (◇) denotes HPV-HNSCC.

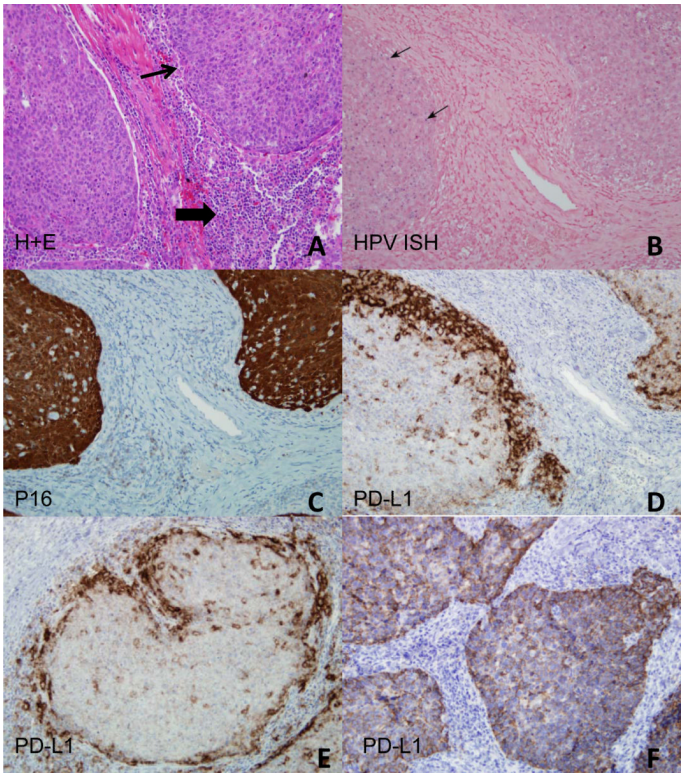

Figure 3. High levels of PD-L1 expression present in the tumor microenvironment of HPV-HNSCC

A. Hematoxylin and eosin stain of HPV-HNSCC demonstrates the proto-typic tumor nests (depicted by thin arrow) surrounded by a dense inflammatory stroma (depicted by thick arrow). Serial sections evaluated for **B**, HPV ISH (arrows mark areas of blue, intranuclear staining); **C**, p16 IHC; and **D-F**, PD-L1 IHC. Two patterns of PD-L1 staining were observed: peripheral tumoral staining (**D, E**) and diffuse intratumoral staining (**F**). Magnification, 400x

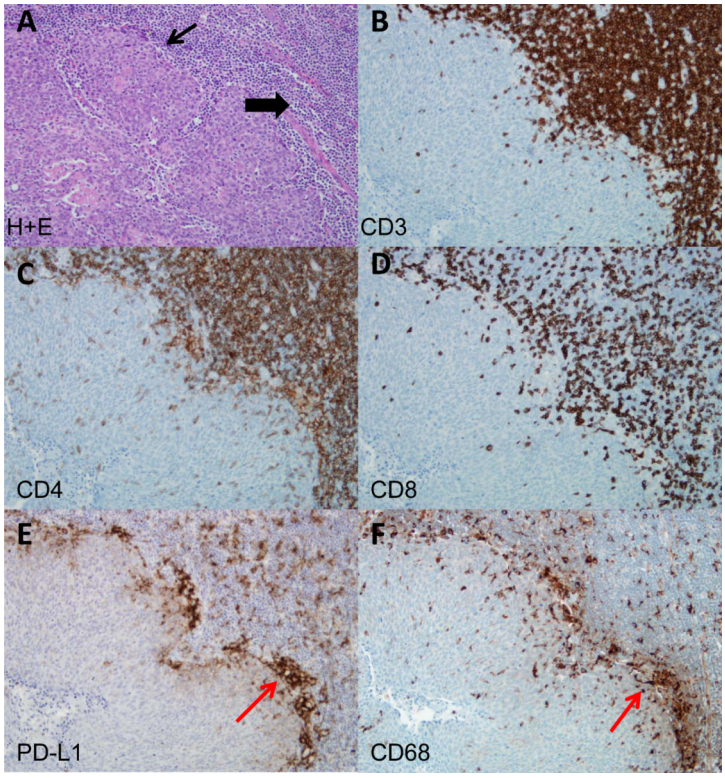

Figure 4. Co-localization of TILs with PD-L1 expression in HPV-HNSCC

A. Hematoxylin and eosin stain of HPV-HNSCC (thin arrow marks tumor nests and thick arrow marks inflammatory stroma). Serial sections evaluated for: **B**, CD3; **C**, CD4; **D**, CD8; **E**, PD-L1; and **F**, CD68 expression. Red arrows indicate a representative area with clusters of PD-L1 and CD68 expression in serial sections (**E, F**). Magnification, 400x.

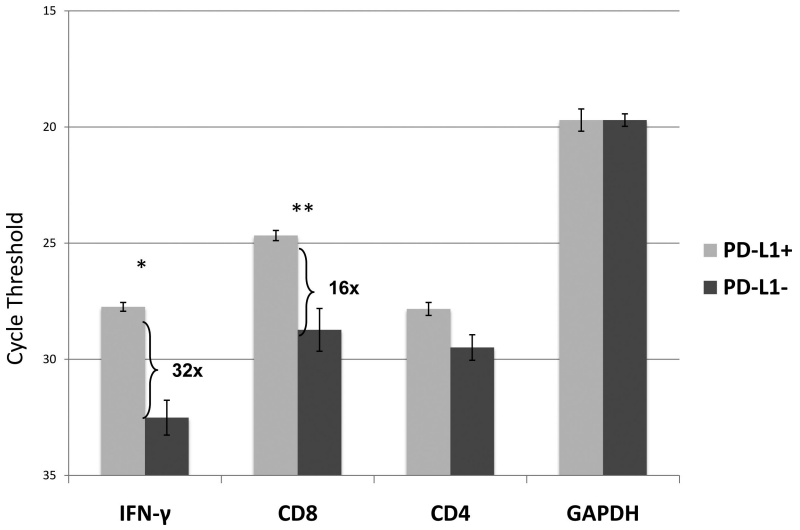

Figure 5. Increased expression of IFN-γ and CD8 mRNA in PD-L1(+) vs. (-) tonsil cancers

IFN-γ, CD8, CD4, and GAPDH were evaluated by quantitative RT-PCR in both PD-L1(+) (n=3) and PD-L1(-) (n=6) tumors . Error bars represent standard error of the mean. Cycle threshold is on a log2 scale; lower numbers indicate greater expression. *p=0.003. **p=0.002. Results are representative of two separate experiments.

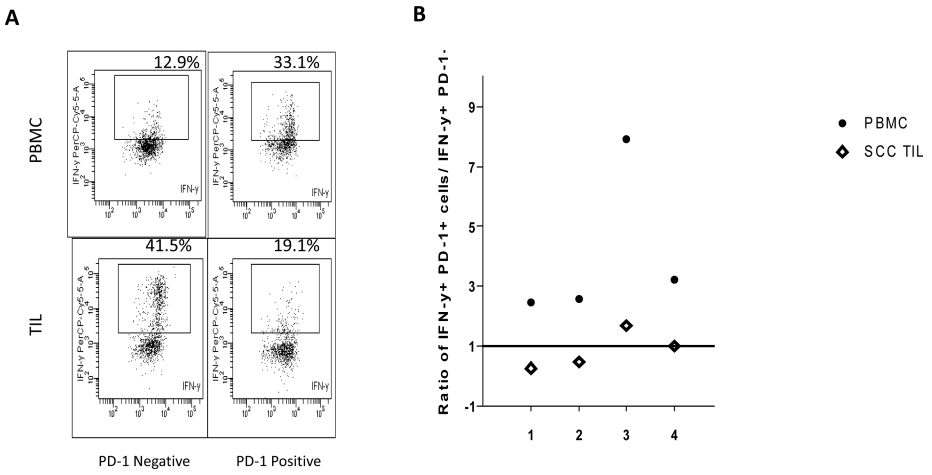

Figure 6. PD-1 expressing CD8+ TILs are functionally anergic relative to peripheral blood PD-1 expressing T cells

A. Representative flow cytometry comparing IFN-γ production by CD8+ T cells sorted by PD-1expression in PBMCs and TILs and stimulated with PMA/ionomycin. **B**. Summary graph of the ratio of IFN-γ production by PD-1(+) to PD-1(-) TILs and peripheral blood, in response to PMA/ionomycin. A value greater than 1 indicates increased IFN-γ production in PD-1(+) compared to PD-1(-) T cells, and a value less than 1 indicated a reduction. (•) denotes PBMC and (◇) denotes TILs.

Table 1

PD-L1 Expression in Head and Neck Cancers

	HPV (+) (N=20)		HPV (-) (N=7)	
	Positive	**Negative**	**Positive**	**Negative**
PD-L1 Expression	14/20 (70%)	6/20 (30%)	2/7 (29%)	5/7 (71%)
Membranous Staining	14/14 (100%)	-	2/2 (100%)	-
Tumor Periphery	13/14 (93%)	-	2/2 (100%)	-
Diffuse within Tumor	1/14 (7%)	-	-	-
Presence of TILs	14/14 (100%)	3/6 (50%)	2/2 (100%)	2/5 (40%)